AD-A090 532 PACIFICA TECHNOLOGY DEL MAR CA F/G 14/2
STRESS LEVEL INDICATOR FOR REAL-TIME, IN-SITU STRESS GAUGE CALI--ETC(U)
AUG 79 E S GAFFNEY, P L RIERSGARD DNA001-78-C-0177
UNCLASSIFIED PT-U79-0372 DNA-5252F NL

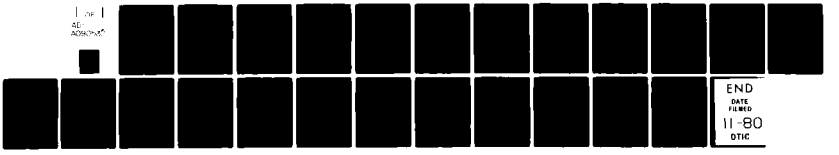

END
DATE FILMED
11-80
DTIC

DNA 5252F

STRESS LEVEL INDICATOR FOR REAL-TIME, IN-SITU STRESS GAUGE CALIBRATION

LEVEL II

(12)

Pacifica Technology
P.O. Box 148
Del Mar, California 92014

29 August 1979

Final Report for Period February 1978—March 1979

CONTRACT No. DNA 001-78-C-0177

APPROVED FOR PUBLIC RELEASE;
DISTRIBUTION UNLIMITED.

DTIC
ELECTE
OCT 1 6 1980
S D
E

THIS WORK SPONSORED BY THE DEFENSE NUCLEAR AGENCY
UNDER RDT&E RMSS CODE B344078462 J11AAXSX35255 H2590D.

Prepared for
Director
DEFENSE NUCLEAR AGENCY
Washington, D. C. 20305

80 10 9 121

Destroy this report when it is no longer needed. Do not return to sender.

PLEASE NOTIFY THE DEFENSE NUCLEAR AGENCY, ATTN: STTI, WASHINGTON, D.C. 20305, IF YOUR ADDRESS IS INCORRECT, IF YOU WISH TO BE DELETED FROM THE DISTRIBUTION LIST, OR IF THE ADDRESSEE IS NO LONGER EMPLOYED BY YOUR ORGANIZATION.

UNCLASSIFIED

SECURITY CLASSIFICATION OF THIS PAGE (When Data Entered)

REPORT DOCUMENTATION PAGE

READ INSTRUCTIONS BEFORE COMPLETING FORM

1. REPORT NUMBER: DNA 5252F	2. GOVT ACCESSION NO.: AD-A090532
3. RECIPIENT'S CATALOG NUMBER:	
4. TITLE (and Subtitle): STRESS LEVEL INDICATOR FOR REAL-TIME, IN-SITU STRESS GAUGE CALIBRATION	5. TYPE OF REPORT & PERIOD COVERED: Final Report for Period Feb 78—Mar 79
6. PERFORMING ORG. REPORT NUMBER: PT-U79-0372	
7. AUTHOR(s): E. S. Gaffney, P. L. Riersgard, N. G. McCaffrey	8. CONTRACT OR GRANT NUMBER(s): DNA 001-78-C-0177
9. PERFORMING ORGANIZATION NAME AND ADDRESS: Pacifica Technology, P.O. Box 148, Del Mar, California 92014	10. PROGRAM ELEMENT, PROJECT, TASK AREA & WORK UNIT NUMBERS: Subtask J11AAXSX352-55
11. CONTROLLING OFFICE NAME AND ADDRESS: Director, Defense Nuclear Agency, Washington, D.C. 20305	12. REPORT DATE: 29 August 1979 13. NUMBER OF PAGES: 24
14. MONITORING AGENCY NAME & ADDRESS (if different from Controlling Office)	15. SECURITY CLASS (of this report): UNCLASSIFIED 15a. DECLASSIFICATION/DOWNGRADING SCHEDULE

16. DISTRIBUTION STATEMENT (of this Report)

Approved for public release; distribution unlimited.

17. DISTRIBUTION STATEMENT (of the abstract entered in Block 20, if different from Report)

18. SUPPLEMENTARY NOTES

This work sponsored by the Defense Nuclear Agency under RDT&E RMSS Code B344078462 J11AAXSX35255 H2590D.

19. KEY WORDS (Continue on reverse side if necessary and identify by block number)

Stress Gauges
Phase Changes
Cerium
Dropbar

20. ABSTRACT (Continue on reverse side if necessary and identify by block number)

A dropbar system has been developed to produce stress pulses above 1 GPa with durations of about 500μs. These pulses are of similar shape and amplitude to those encountered in large explosive tests. This system was to have been used to test a stress level indicator based on the electronic phase transition which occurs in cerium metal; however, due to the extreme reactivity of Ce, no gauges could be constructed. We observed reactions with epoxy over a period of several days which may explain the erratic results of a previous study.

DD FORM 1 JAN 73 1473 EDITION OF 1 NOV 65 IS OBSOLETE

UNCLASSIFIED

SECURITY CLASSIFICATION OF THIS PAGE (When Data Entered)

TABLE OF CONTENTS

LIST OF ILLUSTRATIONS

1. Introduction

A dropbar system has been developed to produce stress pulses above 1 GPa with durations of about 500 μs. These pulses are of similar shape and amplitude to those encountered in large explosive tests. This system was to have been used to test a stress level indicator based on the electronic phase transition which occurs in cerium metal; however, due to the extreme reactivity of Ce, no gauges could be constructed. We observed reactions with epoxy over a period of several days which may explain the erratic results of a previous study.

We recommend that future work on stress level indicators exclude Ce because of its high reactivity. Among the metals, $Tl_{.77}In_{.23}$ and $BiSn_2$ both have phase changes below 1 GPa and warrant further study. Another interesting class of metal phase transitions are melting transitions many of which have pressure dependence such as Ga, Hg, Hg-Tl and Rb-Na. Semi-conductor metal transitions should also be investigated.

2. Background

Design of hardened underground structures for defense relies on accurate constitutive models of the rocks or soil surrounding such structures. The principle sources of data for these models are small laboratory tests and large field tests. However, confidence in the data thus obtained has been slow to develop because of uncertainties in the effects of scale on rock properties, on the one hand, and in the calibration of stress gauges used in field tests, on the other. This research and development project was undertaken to provide a real-time, *in situ* calibration technique for stress gauges. The objective was to produce an electrical signal in the form of a box car fuction whose upward and downward edges would correspond to known stress levels. A subsidiary objective was to develop a gauge calibration facility where gauges to be used in the field could be subjected to transient stress pulses of an amplitude and duration typical of those encountered in field testing.

The difficulties of credibly calibrating piezoresistive stress gauges are familiar to anyone who has used them. The two most commonly used metals are manganin and ytterbium (Yb). The piezoresistive coefficient of both metals depends on whether the material has been hot-worked such as drawn wire and hot-rolled foil, cold-worked as is the case of most foils, or annealed. Furthermore both materials may exhibit hysteresis, a different response to a given stress depending on whether the stress is increasing or decreasing. The measured resistance can also be changed by simple geometric changes at zero stress such as stretching or puncturing. Therefore, a need exists for a technique to provide real time, in situ calibration for such gauges when they are to be installed in field tests. One would like, for instance, an indicator based on a phenomenon that depends on stress alone and not on strains or metallurgical history.

The approach to the main objective was one used by Physics International (PI) from 1974 to 1977[1]. The basis of their work was the existence of phase changes in a wide variety of materials including both metals and insulators. Literally hundreds of phase changes have been found to occur in a wide variety of materials when they are subjected to high pressures. The work of Bridgman[2-5] is by far the most extensive by a single investigator in this area, but numerous other workers can also be cited[6-8].

The properties that an ideal stress level indicator phase change should have can be described as follows: (1) The phase change should be rapid, reproducible and reversible (but not necessarily at the same pressure), resulting in a large, discontinuous change in a measureable physical property. (2) The pressure of the phase change and the magnitude of the discontinuity should be independent of temperature. (3) The material should be readily available, non-hazardous, and relatively stable under normal conditions of atmosphere, temperature and humidity. Probably no material meets all of these requirements for ideality; in order to be successful the first criterion must be met, at least. As we shall see, none of the metals investigated by PI fully meet the second and third criteria.

The study of PI concentrated on two particular types of phase changes - transitions in metals exhibiting a discontinuity in electrical resistivity and transitions in dielectrics exhibiting a discontinuity in specific volume and dielectric constant which could lead to a capacitance change.

After surveying 26 materials, they selected four metals (Bi, Ce, $Tl_{.77}In_{.23}$, Bi_3Pb), one semiconductor (HgSe), and five insulators (KNO_3, NH_4I, ortho-nitrochlorobenzene, camphor and thiourea). After a series of gas gun tests, PI recommended Bi, Bi_3Pb, Ce, thiourea and NH_4I for further study. These materials experience phase transitions at about 2.6 GPa, 2.5 GPa (loading)/0.5 GPa (unloading), 700 MPa, 350 MPa and 50 MPa, respectively. HgSe and Tl/In are both toxic and the conductivity of the Tl/In alloy is too high to make a good gauge.

Selection of a material for further investigation from the PI subset was constrained by two further considerations. First, thiourea and NH_4I were rejected because it was felt that resistivity measurements presented fewer experimental problems than capacitance measurements. The subsidiary objective of developing a facility for calibration of field gauges led to tne rejection of the two Bi materials because the high pressures required could not be obtained in a drop bar apparatus. Given these constraints, cerium was selected as the material for further investigation.

Cerium exists in a face centered cubic (α) phase at 300K and 0.1 MPa. However, when cooled below about 263K it begins to invert to a hexagonal close packed (β) structure, and below about 100K inverts to a second face centered (α') structure 13.5 per cent denser than the α structure. The difference between the α and α' structures is attributed to an electronic transition between the 4f and 5d subshells of the Ce atom and is accompanied by a marked decrease in resistivity of Ce. None of these transitions is isothermal; the ratio of α to β or β to α' varies continuously over a range of temperature of up to 40K. Furthermore, there is a definite hysteresis depending on whether temperature is increasing or decreasing. It is also seen that working above 263K facilitates the β to α transition and working below 77K facilitates both the β to α' and α to α' transitions.

Bridgman[2,3] observed a phase transition and a resistivity change at 0.7 GPa in Ce, and Lawson and Tang[6] determined that the high pressure phase, at 1.5 GPa and room temperature, had a face centered structure with nearly the same lattice constant as the α' phase. Herman and Swenson[7] later made volume measurements at various pressures and showed that the high pressure phase is continuous with the low temperature α' phase. A hysteresis of almost 0.2 GPa was observed between loading and unloading. The P-T phase diagram of Ce based on their work is shown in Figure 1. The high pressure extension of the $\alpha - \beta$ transitions is purely conjectural. To further complicate matters, Swenson[8] has suggested that, at about 1.8 GPa and 600K, there is a critical point at which the α and α' phases are indistinguishable.

Based on the static pressure measurements, Ce hardly appears to be a likely candidate for a stress indicator, especially in view of the sluggish, continuous nature of the phase transitions. However, the fact that working the material seems to facilitate equilibrium is perhaps encouraging. In fact, the PI studies may be interpreted as showing that the phase change can procede at least to the extent of 20 to 30 per cent α converted to α' in a loading time of less than 0.5 μs. However, the phase transition was not observed in all tests in which it should have occurred. Their published results are not adequate to determine closely the pressure of the observed transition.

3. Experimental Techniques

3.1 Dropbar Facility

Dropbar techniques have been used for several years to test and calibrate a variety of ground shock instruments[9-12]. Dropbars have been reliable tools for producing controlled reproducible stress profiles with durations of 0.5 to 12 ms, durations similar to those encountered in many field applications. The shape of the stress pulse can be predetermined by the variation along the bars axis of its cross-section. The duration of the pulse (T) is the time required for the stress pulse to propagate up and down the bar of length L,

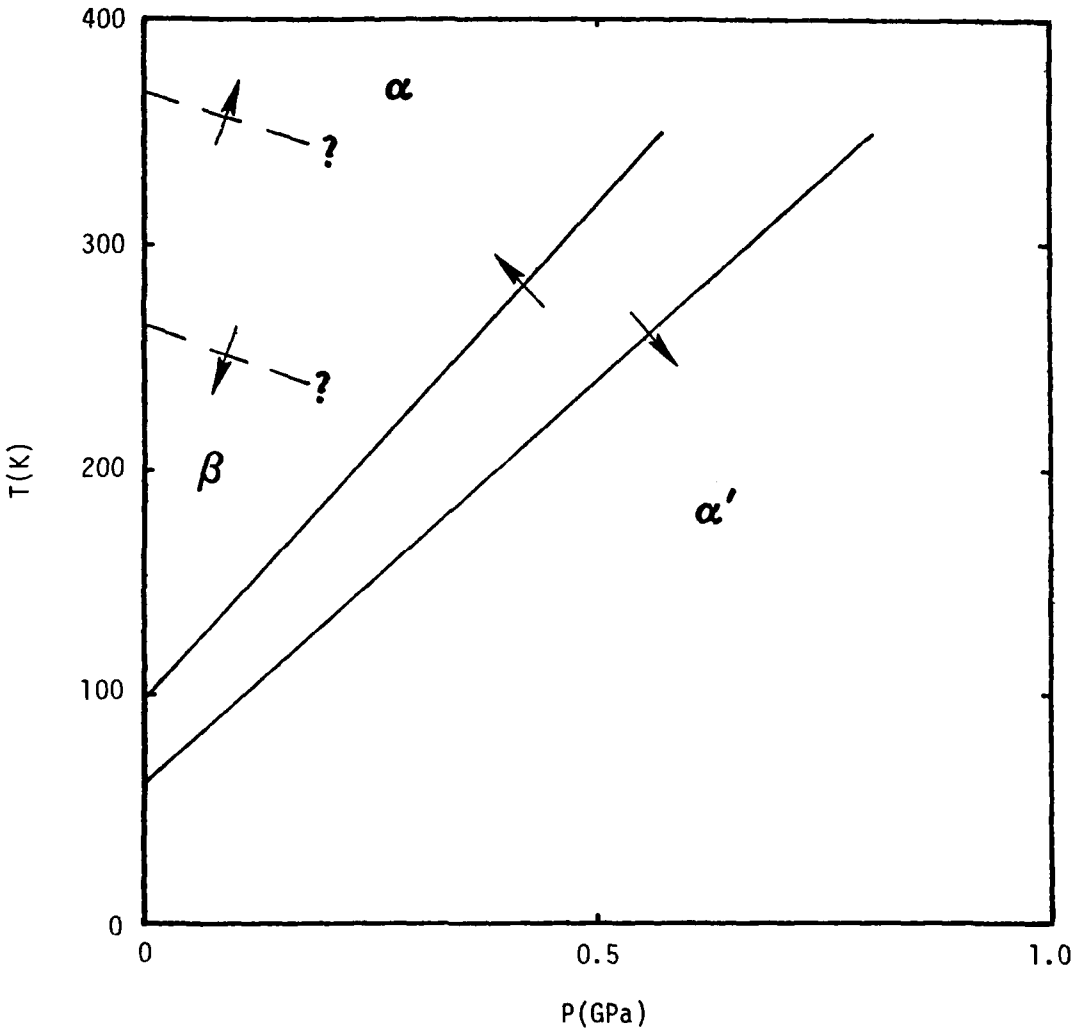

Figure 1. Phase diagram for Ce. All transitions are hysteretic. Arrows indicate direction of transition.

$$T = \frac{2L}{V} \quad ,$$

where V is the wave speed. In our case the bars was always below its yield point so $V = E/\rho$, the rod wave velocity, where E is Young's modulus and ρ is the density. The shape of the stress pulse, $\sigma(t)$, is related to the shape of the bar, in terms of its cross-section, A(x), by the approximate relation

$$\sigma(t) \approx k\, C_i A(\tfrac{1}{2} TV) \qquad (1)$$

where C_i is the impact speed of the bar and $k = \rho V/A^*$ with A^* being the area in the gauge plane which supports the bar. In actual practice there is dispersion in the wave propagation so that $\sigma(t)$ will be a smoothed version of A(x).

In our tests we planned to use Ce gauge elements about 2 cm square so that a large A^* would be required. This necessitated the construction of a larger dropbar facility than used in previous tests. Furthermore, it was desired to work with peak stresses up to 1.5 GPa which necessitated use of a hardened steel bar with a yield strength in excess of that value (220 ksi) and an impact velocity of about 10 ms^{-1}. One other requirement was that tne stress should pass through the Ce phase transition gradually (about 10^4GPa s^{-1} or less) so that the effect of loading rate on the sharpness of the phase transition could be observed.

Based on these requirements we designed a dropbar as shown in Figure 2. The bar is a 0.1016 m diameter round bar of 300 M (var) steel, machined as shown, with an impact diameter of 47.9 mm, and hardened to Rockwell C52 (yield~ 220 ksi). The flat and flag on one side were machined to permit use of a velocity detector described below.

In order to achieve an impact velocity of 10 m/s using free fall at 10 m s^{-2} a height of about 5 m was required. The dropbar system was constructed by modifying an existing 30 ft (9 m) drop tower at a nearby plant. The bar

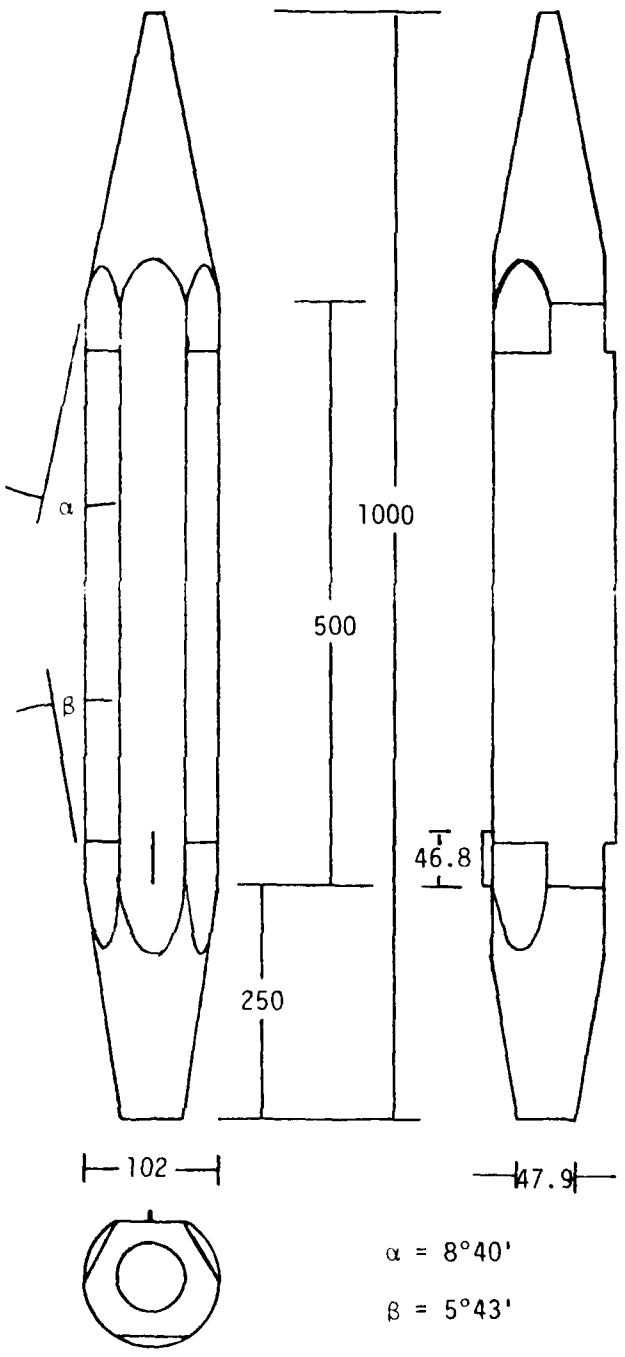

Figure 2. Drop bar used to produce calibration pulses. Dimensions are in millimeters.

is suspended from a cable by a remotely operated catch. The bar is guided to the impact point by three pairs of trolleys which run on three vertical rods which are strapped together at frequent intervals for rigidity. The rods are attached to the supporting beam at the top and bottom.

The velocity of the bar is determined by measuring the time required for a flag of known length (46.8 mm) to traverse a light beam. This is monitored by coupled GaAs infra-red emitting diode and silicon photo-transistor (TIL138) mounted on the lower support bar of the guide rods. The flag is 1 mm thick while the gap of the sensor is 3.1 mm, permitting a ± 1 mm alignment error for the bar. The velocity of the bar is measured both downward and upward on the first rebound. This permits calibration of the gauge as described in Section 4.1.

3.2 Ce Gauges

The Ce gauges were designed to be a grid with a length of 90 mm in an area of 100 mm^2. Our first plan was to etch the grid out of thin foils mounted on a mylar substrate using procedures described by PI[1]. The thinnest commercially available foils were 25 μm thick which would yield a resistance of only 3 Ω if the grid lines were 0.1 mm wide. Although that resistance was only about one tenth that desired it would have been adequate for a laboratory test environment. However, the foils were completely oxidized on receipt. Foils were reordered at a thickness of 0.1 mm which would have yielded a value of about 0.75Ω, a marginally useful gauge. This approach also proved unsuccessful because the foil reacted chemically with the epoxy used to mount it on the substrate. The reaction rate was slow, with about 6 days being required to completely alter the metal. This slow reaction with epoxy may explain the variable results of PI with Ce gauges. Those gauges used within a day or so after first gluing should give positive results (shot 15[1]) whereas those used after several days storage should give negative results (shots 5 and 6[1]).

Because of the difficulties experienced with Ce foils, a second production scheme was devised. We attempted to deposit Ce vapor onto a mylar substrate in a vacuum. Numerous attempts were made with various deposition rates but none were successful. At high disposition rates the substrate either became hot enough to flow or reacted directly with the Ce upon deposition. At low deposition rates the Ce atoms reacted with the residual gases in the sample chamber before deposition. In either case the resulting grid was not a conductor. Attempts to cool the substrate during deposition were also unsuccessful.

3.3 Yb Gauges

Our original plan was to combine Ce gauges and Yb gauges into a single gauge package as shown in Figure 3. The Yb would provide a measure of the stress history for comparison with the output of the Ce gauges. The Yb gauges used were manufactured by S^3. They were of 0.05 mm cold rolled foil backed with 0.25 mm fiberglass and had a nominal resistance of 20 Ω.

The package finally used contained only a single Yb gauge because we were not successful in producing Ce gauges. The Yb gauges were laminated between two 2.5 mm sheets of 4130 steel hardened to Rockwell C40. The laminated package was held together by bolts around the edges. The resulting gauge package survived repeated loads up to 1 GPa on the dropbar.

3.4 Data Acquisition and Analysis

The gauges were powered by a pulsed power supply manufactured by S^3, which effectively produced a constant current through a 100 Ω resistor in series with the gauge. The effective circuit is shown in Figure 4. The voltage drop across the gauge was read with a Nicolet Explorer 3 digital storage oscilloscope. After each shot the memory of the scope was read onto tape for later processing.

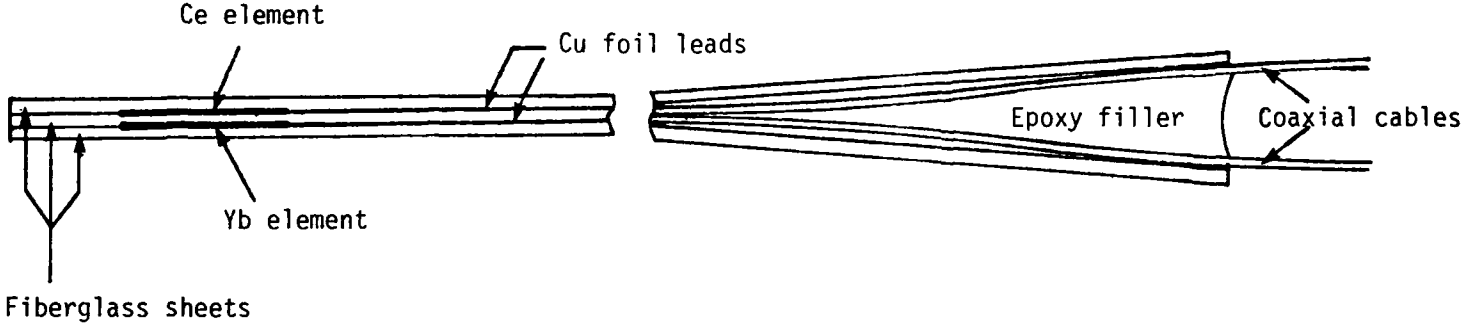

Figure 3. Planned configuration of dual transducer (Ce/Yb) stress gauge.

Voltage records were converted to relative resistance in accordance with the circuit of Figure 4,

$$\frac{\Delta R(t)}{R_0} \equiv \frac{R(t)-R_o}{R_0} = \frac{R_0[R_1+R_0][V(t)-V_0]}{V_0[R_1+R_2] - V(t)R_0} \tag{2}$$

R_0 is the initial gauge resistance, R_1 is the series resistance, V_0 is the initial rise in voltage, and V(t) and R(t) are the measured voltage and the resistance, respectively, at time t.

Relative resistance records were then converted to stress by two techniques. In the first the equations of Ginsberg et al.[2] were used:

$$\sigma = .1082\ [1-\exp(-20.8\Delta R/R_0)] + .9168\Delta R/R_o \tag{3}$$

for loading and

$$\sigma = \sigma_{pk} - \frac{R_{pk} - R}{R_{pk} - R_f} \tag{4a}$$

for unloading where σ_{pk} is the peak stress from equation (3), R_{pk} is the resistance at peak stress and R_f is

$$R_f = R_0 + \Delta R_H = R_0\ (1.1179 + 0.0542\ \ln \sigma_{pk}). \tag{4b}$$

In the second technique the change in momentum of the bar is related to the impulse at the gauge plane, with the further assumption that the relation between $\Delta R/R_0$ and σ is bilinear, that is, linear on both loading and unloading with a different proportionality constant,

$$M(C_i+C_r) = k_1 \int_{t_o}^{t_{pk}} \frac{R(t)-R_o}{R_o}\, dt + k_2 \int_{t_{pk}}^{t_f} \frac{R(t)-R_f}{R_f}\, dt \quad .$$

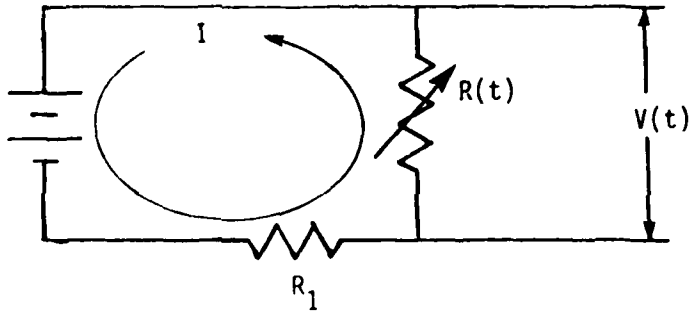

Figure 4. Effective circuit used for reduction of data. R(t) is the piezoresistive transducer.

where C_r is the rebound speed of the bar, k_1 and k_2 are the proportionality constants for loading and unloading respectively, and t_0, t_{pk} and t_f are the times of start of pulse, peak stress and end of pulse, respectively. Using $k_1(R_{pk}-R_0)/R_0=\sigma_{pk}=k_2(R_{pk}-R_f)/R_f$ one of the constants can be eliminated to get

$$\sigma(t) = \begin{cases} \dfrac{R(t)-R_o}{R_o} \dfrac{M(C_c+C_r)}{A^*K} & , t \leq t_{pk} \\ \dfrac{R(t)-R_f}{R_o} \dfrac{M(C_c+C_r)}{A^*K} \dfrac{R_{pk}-R_o}{R_{pk}-R_f} & , t \geq t_{pk} \end{cases} \tag{5}$$

with

$$K = \int_{t_o}^{t_{pk}} \frac{R(t)-R_o}{R_o}\, dt + \frac{R_{pk}-R_o}{R_{pk}-R_f} \int_{t_{pk}}^{t_f} \frac{R(t)-R_f}{R_f}\, dt$$

The principle difficulty with equation (5) is that A^* is not accurately known for the flat pack gauge design. Data obtained below are reported assuming A^* is equal to the impact surface, 1.802×10^{-3} m^2.

4. Results and Discussion

4.1 Dropbar Tests

Figure 5 shows $\Delta R/R_0$ vs. time for three typical dropbar tests at about 0.3 GPa, 0.5 GPa and 1.0 GPa. In general, they have the desired characteristics of peak stress, duration and loading rate. Shots 6 and 7 do not exhibit the flat top expected (Figure 2) and observed in shot 4. This is probably due to excessive interaction of the bar with the guide rod caused by loosening of the trolley tracks which produced failure to trigger on shot 8. However, the stress pulses are certainly of the correct shape for calibration of gauges to be used in large explosive tests.

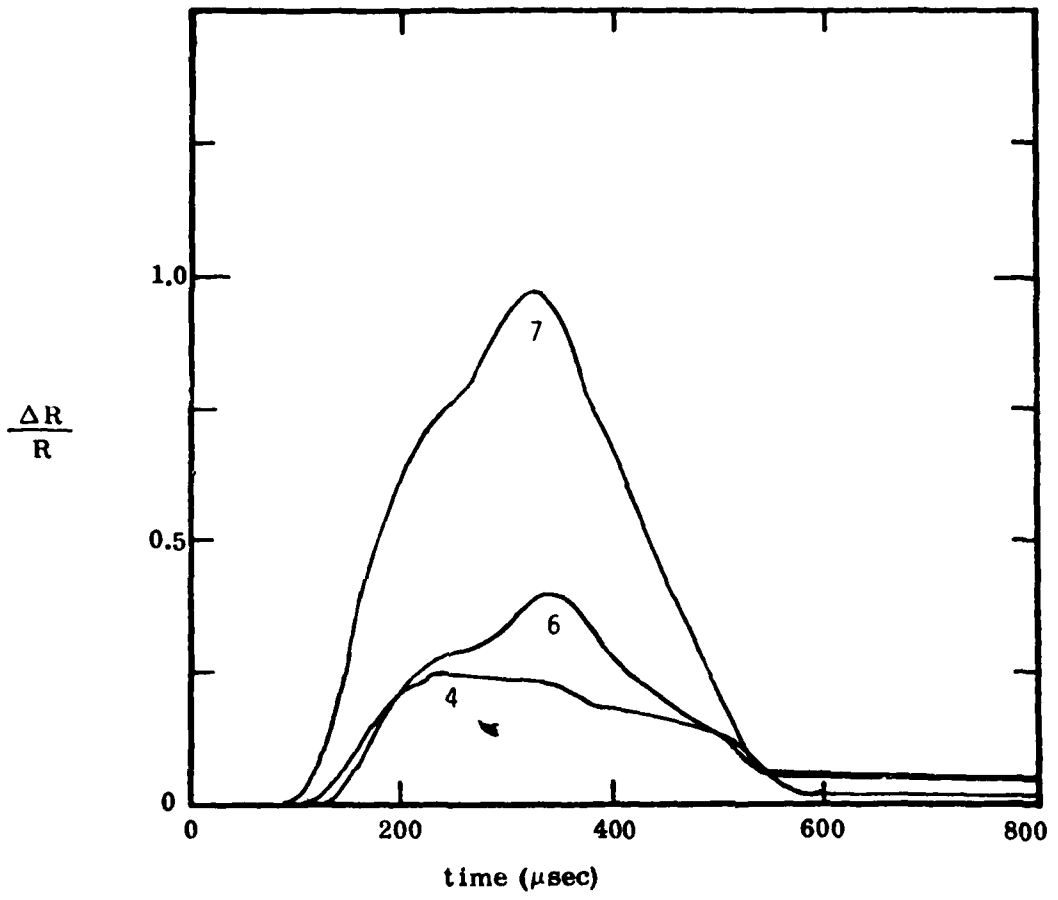

Figure 5. Relative resistance (ΔR/R) as a function of time for three typical tests with peak stresses of about 0.3, 0.5 and 1.0 GPa. Shot numbers are shown below peaks.

Table 1 compares values for peak stress derived from equations (1), (3) and (5). The lack of agreement is striking. The values of equation (3) are to be preferred because the value of A^* is uncertain. Furthermore, derivation of both equations (1) and (5) assume that the stress is distributed uniformly over the area A^*; however, using the solution of Boussinesq for the stress in a half space subjected to a circular load[13] we have

$$\sigma(r) = 1/2\ a\ P_{avg}/\sqrt{a^2-r^2}$$

so that $\sigma(r=0)=1/2\ P_{avg.}$ When yielding at the edge of the load is taken into account $\sigma(r=0)$ will be somewhat higher, perhaps between 1/2 Par and 2/3 Par. Thus the values in (1) and (3) should be high by about 1-1/2 to 2 times, as they are. This difficulty could be eliminated by machining a ring out of the gauge to eliminate the coupling to the sides. The resulting gauge might be simpler to calibrate but perhaps less durable.

The hysteresis shown in all the Yb gauges is considerably less than that observed by Ginsberg *et al*[12] given by equation (4b). There are two reasons for this. The very stiff packaging apparently reduces plastic working of the gauge and hence lowers the hysteresis. Furthermore, only shot 6 had a virgin gauge. In shot 4 the gauge had been loaded three times to about the same level during the preceding hour. Shot 7 used the same gauge as shot 6 after a delay of 5 to 10 minutes. It has been shown that hysteresis in Yb is virtually eliminated during repeated loadings[12].

4.2 Ce Gauges

We were not successful in producing any Ce gauge due to the extreme reactivity of the metal. We observed reaction with epoxy over a period of several days which may explain why, in earlier studies, some gauges worked while others did not.

Table 1. Peak stresses in Figure 5 using different equations.

Test	$(\Delta R/R_o)_{max}$	Stress (GPa)		
		eq.(1)	eq.(3)	eq.(5)
4	0.25	716	328	565
6	0.40	1011	450	1050
7	0.95	1510	987	1460

References

[1] K. Seifert and J. Shea, In situ stress gauge calibration, DNA4254F (1977).

[2] P.W. Bridgman, Proc. Amer. Acad. Arts Sci. 76, 55 (1948).

[3] P.W. Bridgman, Proc. Amer. Acad. Arts Sci. 81, 167 (1952).

[4] P.W. Bridgman, Pr.c. Amer. Acad. Arts Sci. 84, 43 (1955).

[5] P.W. Bridgman, Proc. Amer. Acad. Arts Sci. 82, 71 (1953).

[6] A.W. Lawson and L.Y. Tang, Phys. Rev. 76, 301 (1949).

[7] R. Herman and C.A. Swenson, J. Chem. Phys. 29, 398 (1958).

[8] C.A. Swenson, Solid State Phys. 11, 41 (1960).

[9] H.D. Glenn, Diagnostic techniques improvement program - high explosive development phase, DNA2987T (1972).

[10] D.R. Grine and P.L. Coleman, Ground motion gauge development, DNA3524T (1974).

[11] P. Coleman, W. Ginn and D. Grine, Ground motion gauge development, DNA3702F (1975).

[12] M.J. Ginsberg, D.E. Grady, P.S. DeCarli and J.T. Rosenberg, Effects of stress on the electrical resistance of ytterbium and calibration of ytterbium stress transducers, DNA 3577F (1973).

[13] S.P. Timoshenko and J.N. Goodier, Theory of Elasticity, McGraw-Hill, New York (1970), p. 408.

DISTRIBUTION LIST

DEPARTMENT OF DEFENSE

Assistant to the Secretary of Defense
Atomic Energy
ATTN: Executive Assistant

Defense Advanced Rsch. Proj. Agency
ATTN: TIO

Defense Nuclear Agency
ATTN: SPAS
ATTN: SPSS, T. Deevy
ATTN: SPTD
4 cy ATTN: TITL

Defense Technical Information Center
12 cy ATTN: DD

Field Command
Defense Nuclear Agency
ATTN: FCT
ATTN: FCPR

DEPARTMENT OF THE ARMY

Atmospheric Sciences Laboratory
U.S. Army Electronics R & D Command
ATTN: DELAS-EO

BMD Advanced Technology Center
Department of the Army
ATTN: ATC-T

BMD Systems Command
Department of the Army
ATTN: BMDSC-NW
ATTN: BDMSC-H

Chief of Engineers
Department of the Army
ATTN: DAEN-ZCM

Harry Diamond Laboratories
Department of the Army
ATTN: DELHD-I-TL

U.S. Army Ballistic Research Labs
ATTN: DRDAR-BLT
ATTN: DRDAR-BLE
ATTN: DRDAR-BLV
ATTN: DRDAR-TSB-S

U.S. Army Engr Waterways Exper Station
ATTN: WESSD
ATTN: WESGR
ATTN: WESSA
ATTN: WESSE
ATTN: WESGH
ATTN: WESSS

U.S. Army Material & Mechanics Rsch Ctr
ATTN: DRXMR-HH

DEPARTMENT OF THE ARMY (Continued)

U.S. Army Materiel Dev & Readiness Cmd
ATTN: DRXAM-TL

U.S. Army Missile Command
ATTN: RSIC

U.S. Army Nuclear & Chemical Agency
ATTN: Library for ATCA-NAW

U.S. Army Satellite Comm Agency
ATTN: Technical Library

U.S. Army Training and Doctrine Comd
ATTN: ATORI-OP
ATTN: ATCD-T

White Sands Missile Range
Department of the Army
ATTN: STEWS-FE-R

DEPARTMENT OF THE NAVY

David Taylor Naval Ship R & D Ctr
ATTN: Code 17

David Taylor Naval Shir R & D Ctr
ATTN: Code 770

Headquarters
Naval Material Command
ATTN: MAT-0323

Naval Research Laboratory
ATTN: Code 2627

Naval Sea Systems Command
ATTN: SEA-0352

Naval Surface Weapons Center
ATTN: Code E21
ATTN: Code R15
ATTN: Code F31
ATTN: Code K06

Naval Weapons Center
ATTN: Code 31707

Office of Naval Research
ATTN: Code 715

DEPARTMENT OF THE AIR FORCE

Aeronautical Systems Division
Air Force Systems Command
ATTN: ASD/ENFTV

Air Force Flight Dynamics Laboratory
ATTN: FXG

Air Force Geophysics Laboratory
ATTN: LY

DEPARTMENT OF THE AIR FORCE (Continued)

Air Force Institute of Technology
ATTN: LIBRARY

Air Force Materials Laboratory
ATTN: LPH
ATTN: MAS
ATTN: MBE
ATTN: MBC

Air Force Weapons Laboratory
Air Force Systems Command
ATTN: DYS
ATTN: SAB
ATTN: DYT
ATTN: DYV
ATTN: SUL
ATTN: NTO

DEPARTMENT OF ENERGY

Department of Energy
ATTN: OMA/RD&T

OTHER GOVERNMENT AGENCY

Federal Emergency Management Agency
ATTN: Asst Dir for Rsch, J. Buchanon

DEPARTMENT OF DEFENSE CONTRACTORS

Aerospace Corp.
ATTN: R. Crolius
ATTN: J. McClelland

AVCO Research & Systems Group
ATTN: Document Control

Boeing Co.
ATTN: R. Holmes
ATTN: M/S 85/20, E. York
ATTN: R. Dyrdahl

General Electic Company-TEMPO
ATTN: DASIAC

DEPARTMENT OF DEFENSE CONTRACTORS (Continued)

General Electric Company-TEMPO
ATTN: G. Perry

General Electric Company-TEMPO
ATTN: E. Bryant

General Research Corp.
ATTN: T. Stathacopoulos

Kaman Sciences Corp.
ATTN: D. Sachs

Physics International Co.
ATTN: Technical Library

R & D Associates
ATTN: P. Haas

Science Applications, Inc.
ATTN: O. Nance
ATTN: D. Hove

SRI International
ATTN: A. Burns
ATTN: G. Abrahamson
ATTN: H. Lindberg

Systems, Science & Software, Inc.
ATTN: R. Duff

Teledyne Brown Engineering
ATTN: R. Patrick

Terra Tek, Inc.
ATTN: S. Green

TRW Defense & Space Sys Group
ATTN: N. Lipner

TRW Defense & Space Sys Group
ATTN: P. Dai
ATTN: R. Mortensen

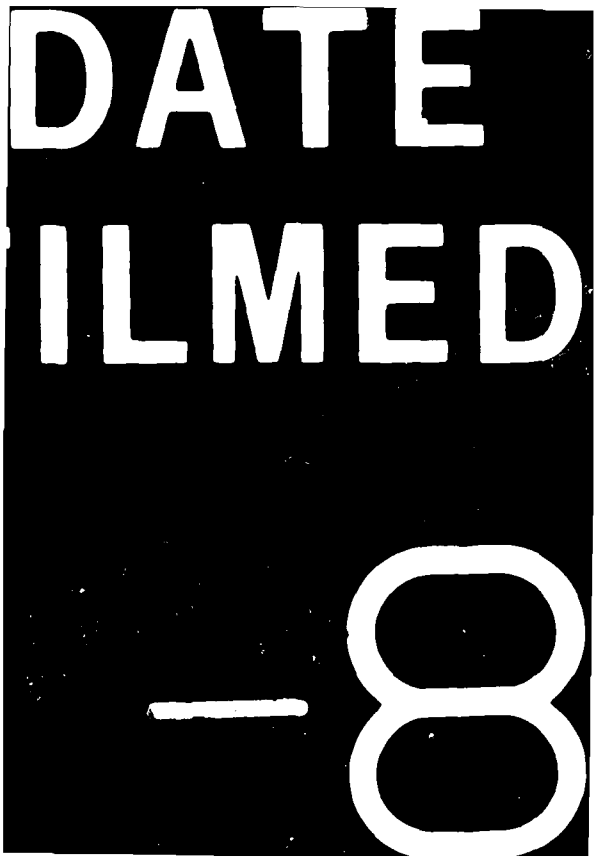
DATE
ILMED
-8